



# An Active Power Factor Corrected Power Supply fed Induction Motor Drive by Controlling the Leakage Inductance for Transformer with Soft Switching Strategy

Jagata Kotasatyavathi<sup>1</sup> | Guduru Ravi Kumar<sup>2</sup>

<sup>1</sup>PG Scholar, Department of EEE, Priyadarshini Institute of Technology & Science, Chintalapudi, India.

<sup>2</sup>Associate Professor & HOD, Department of EEE, Priyadarshini Institute of Technology & Science, Chintalapudi, India.

## To Cite this Article

Jagata Kotasatyavathi and Guduru Ravi Kumar, "An Active Power Factor Corrected Power Supply fed Induction Motor Drive by Controlling the Leakage Inductance for Transformer with Soft Switching Strategy", *International Journal for Modern Trends in Science and Technology*, Vol. 07, Issue 03, March 2021, pp.: 107-114.

## Article Info

Received on 03-February-2021, Revised on 02-March-2021, Accepted on 05-March-2021, Published on 12-March-2021.

## ABSTRACT

Nowadays the use of electronic equipment finds a progressive development in the modern world. Hence it becomes a mandate to check whether the harmonic content of line current of any electronic device which is connected to the ac supply meets the appropriate standards. This demand is satisfied by implementing the Power Factor Correction (PFC) circuit in order to make the input current to be in sinusoidal in nature and in-phase with the input voltage. Numerous solutions are available to make the line current almost sinusoidal. This paper describes an isolated power factor corrected power supply that utilizes the leakage inductance of the isolation transformer to provide boost inductor functionality. The bulk capacitor is in the isolated part of the power supply allowing for controlled startup without dedicated surge limiting components. A control method based on switch timing and input/output voltage measurements is developed to jointly achieve voltage regulation and input power factor control.

**KEYWORDS:** AC-DC power conversion, power factor correction, transformer leakage inductance.

## INTRODUCTION

The widespread use of electronic devices from single-phase ac supplies necessitates thincreasing use of power factorcorrected (PFC) power supplies in many applications includingelectronic equipment, computer servers, and consumer products. PFC power supplies provide low total harmonic distortion(THD) in the current drawn from the line and this is an increasingly important requirement.Power factor correction techniques have been researchedwidely in the literature [1], [2] and an active PFC using highfrequency switching techniques [3] are now commonly used.

The overarching principle involves controlling the input currentdrawn from the mains input to achieve the required current shapefor low THD and high power factor. The power supply must provide a regulated dc output voltage and for many applications,galvanic isolation is also required.The basic boost or step-up converter [4] forms the core ofmost architectures as it has an input inductor that allows inputcurrent control to be readily achieved. The well-known flybackconverter can be derived from the buck-boost converter, but witha transformer for output voltage isolation [4].

Traditionally for PFC supplies, fly back converters have been used for lower power levels ( $\leq 100$  W). For higher power levels ( $\geq 500$  W), a separate boost converter for PFC and separate dc to dc converter with transformer isolation for output dc voltage regulation is used.

### PROPOSED PFC ARCHITECTURE

In this paper, an active PFC power supply is described, whereby the leakage inductance of the high-frequency isolation transformer is used to provide the functionality of the boost inductor. Minimization of the leakage inductance in high frequency isolation transformers is normally desirable in most dc to dc converters, although resonant and soft switching architectures do use a controlled amount of leakage inductance [17] for the purpose of reducing switching losses.

The use of a controlled amount of leakage inductance is proposed in this paper to eliminate the need for two separate magnetic components in the two-stage PFC converter and instead uses one magnetic component to achieve both the power factor correction and galvanic isolation. Inrush current on startup can also be controlled by implementing a soft start strategy whereby the large bulk capacitor is initially charged up in a controlled manner.

Bidirectional core excitation is used, with part of the energy transferred via transformer action, and part stored in the transformer leakage inductance. The described architecture provides a useful technique at power levels above those suitable for single-stage flyback type converters.

The technique lends itself to the adoption of wide band gap semiconductor devices [18] with hard switching [19], [20]. Typically applications might include LED lighting, electronic equipment, server power supplies, and on-board chargers for electric vehicles.

### Proposed Architecture

The circuit diagram of the proposed power supply is shown in Fig. 3.1. A conventional four diode full wave rectifier rectifies the input ac source voltage producing a voltage  $V_R$ . This voltage is inverted to the high frequency  $f_s$  with a half-bridge inverter before being applied to a high-frequency transformer  $T_{xfr}$ . The half-bridge inverter consists of the two switches  $M_1$  and  $M_2$  operated out of phase with a 50% duty cycle at the switching frequency  $f_s$  and the capacitive divider formed by  $C_1$  and  $C_2$ .

The capacitors  $C_1$  and  $C_2$  prevent dc current flowing through the transformer primary and causing saturation problems. The values of  $C_1$  and  $C_2$  are chosen sufficiently small, such that at the mains frequency  $f_{AC}$  and low power level, they allow the rectifier output voltage  $V_R$  to follow the input mains waveform envelope. However, at the switching frequency, their values are sufficiently large to act as fixed voltage sources and not resonate with the transformer inductances or load. For the circuit of Fig. 1. The mains input voltage is  $V_M(t) = \sqrt{2}V_{AC} \sin(2\pi f_{AC}t)$ , with  $V_{AC}$  being the rms input voltage and  $V_R(t)$  being the input voltage fully rectified. The transformer primary voltage  $V_P(t)$  switches at the high frequency rate  $f_s$ , but with an amplitude of half  $V_R(t)$ , due to the half-bridge configuration.

The symbol for the transformer in Fig. 3.1 is drawn to emphasize that the transformer leakage inductance is used in the circuit rather than the usual case whereby leakage inductance is minimized as much as possible. The key to the operation of the circuit is the bidirectional secondary shorting switch shown in Fig. 3.1 [21].

### THEORY OF OPERATION

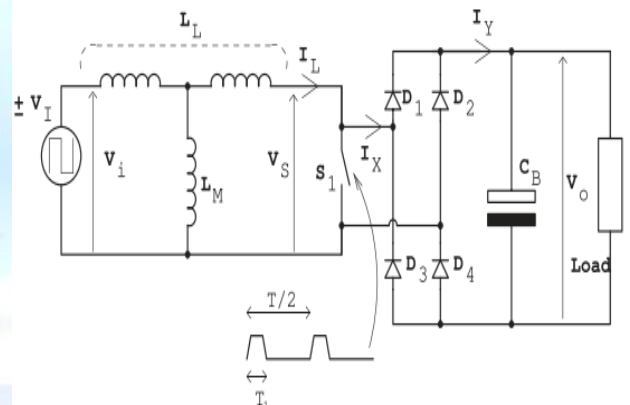


Fig. 2.2. Simplified circuit model for the proposed power supply.

Fig. 2.2 shows a simplified circuit model for the proposed power supply. Assuming the switching frequency of the converter is very high compared to the ac source frequency, the input to the transformer can be considered to be essentially a 50% duty cycle square wave with period  $T$  and peak amplitude  $\pm V_I$ . The model in Fig. 3.2 is referenced to the secondary side of the transformer and the voltage amplitude into the transformer model is the primary voltage  $V_P(t)$  multiplied by the turns ratio of the transformer, or at time  $t = kT$ .

$$V_I[kT] = \left| V_P(kT) \frac{N_s}{N_p} \right| \quad (2.1)$$

The operation of the circuit is based on the assumption that the transformer magnetizing

inductance LM has little effect on the operation of the circuit other than to add a magnetizing current to the input source. Simulations show that magnetizing current is significantly less (a factor of 1.5 × or less), than the currents being transferred, have little impact on the circuit overall functionality. The total leakage inductance of the transformer is denoted as LL and the current flowing out of the transformer secondary winding is denoted as IL(t).

The operation of the system is essentially that of a step up or boost converter and is based around the timing of shorting switch S1 in Fig. 3.2. At the beginning of a switching cycle, the input voltage switches to +VI (dropping the [kT] for notation for clarity) and simultaneously the shorting switch S1 is turned ON. The current IL(t) in the leakage inductance LL rises linearly while the switch S1 is ON. When the switch S1 is turned OFF, the current in the leakage inductance is forced through the rectifier diode bridge formed by D1, D2, D3, and D4, and into the capacitor CB and system load, and the current in the leakage inductance falls. After a period of T2, the input voltage changes sign to -VI and the same operation occurs, except for a change in the sign of the inductor current. Two distinct operation modes of the circuit can be identified depending on whether the leakage inductance current starts at zero and returns to zero before time T2, denoted as the discontinuous conduction mode (DCM), or when the leakage inductance current starts the cycle with a nonzero (negative) value, retains a nonzero (positive) value at time T2 and returns to a nonzero (negative) value at the end of the cycle (time T), denoted as the continuous conduction mode (CCM). To achieve unity power factor, the circuit needs to be operated in such a manner as to control the input current drawn from the supply. The two operating modes are now discussed in detail to relate the input current drawn to the timing period T1.

### Discontinuous Conduction Mode

Fig. 3.3(a) shows the input voltage Vi(t), the secondary voltage VS(t), the leakage inductor current IL(t), and the current into and out of the output rectifier IX(t) and IY(t) as well as the switch current IS1(t), for the circuit operating in DCM. With the shorting switch S1 closed, the leakage inductor current IL(t) rises from zero to the value +IP over the set period T1, thus

$$I_P = V_I T_1 / L_L. \quad (3.2)$$

When the shorting switch S1 opens, the inductor current falls back to zero over a period T2 with the relationship

$$I_P = (V_O - V_I) T_2 / L_L. \quad (3.3)$$

The sum of the periods must be less than the half period T/2 to ensure operation in the DCM or

$$T_1 + T_2 \leq \frac{T}{2}. \quad (3.4)$$

The average input current to the transformer model (ignoring the magnetizing inductance) over the period T/2 can then be calculated as follows:

$$I_L^* = \frac{1}{2} I_P \frac{T_1 + T_2}{\frac{T}{2}} \quad (3.5)$$

And combining with (2) and (3), the average input current is

$$I_L^* = \frac{T_1^2}{T L_L} \left( \frac{V_I V_O}{V_O - V_I} \right). \quad (3.6)$$

The actual input current from the ac source is a scaled version of this current and is

$$I_M = \frac{1}{2} \frac{N_s}{N_p} I_L^* \quad (3.7)$$

With any contribution from the magnetizing inductance averaging to zero over each T period.

It is apparent by considering (1) and (7), that achieving unity power factor in the input source is equivalent to controlling the current value I\*L to be directly proportional to VI. Denoting the constant of proportionality as GM, or IL\* = GM VI, then substituting in (6) and rearranging yields the equation

$$T_1 = \sqrt{G_M T L_L \left( \frac{V_O - V_I}{V_O} \right)}. \quad (3.8)$$

The equation shows that given a constant of proportionality as GM, the required time period T1 can be calculated by knowledge of the system parameters LL and T, measurement of the output voltage VO and calculating VI by measurement of the rectified input source voltage and scaling by a factor of 1/2 NN sp

### 3.3.2 Continuous Conduction Mode

Fig. 3.3(b) shows the input voltage Vi(t), the secondary voltage VS(t), the leakage inductor current IL(t), and the current into and out of the output rectifier IX(t) and IY(t) as well as the switch current IS1(t), for the circuit operating in CCM. With the shorting switch S1 closed, the leakage inductor current IL(t) rises from the value -IE to the value +IP over the set period T1, thus

$$I_P + I_E = V_I T_1 / L_L. \quad (3.9)$$

When the shorting switch S1 opens, the inductor current falls back to +IE over a period T2 = T/2 - T1 with the relationship

$$I_P - I_E = (V_O - V_I)T_2/L_L. \quad (3.10)$$

The average input current to the transformer model (ignoring the magnetizing inductance) over the period T/2 can then be calculated as follows:

$$I_L^* = \frac{\frac{1}{2}(I_P - I_E)T_1 + \frac{1}{2}(I_P + I_E)T_2}{\frac{T}{2}} \quad (3.11)$$

And combining with (9) and (10), the average input current can be shown as

$$I_L^* = \left(T_1 \frac{T}{2} - T_1^2\right) \frac{V_O}{TL_L}. \quad (3.12)$$

With  $I^*L = GM VI$ , then substituting in (12) and rearranging yields the equation

$$T_1 = \frac{T}{4} \left(1 - \sqrt{1 - \frac{16G_M L_L V_I}{TV_O}}\right). \quad (3.13)$$

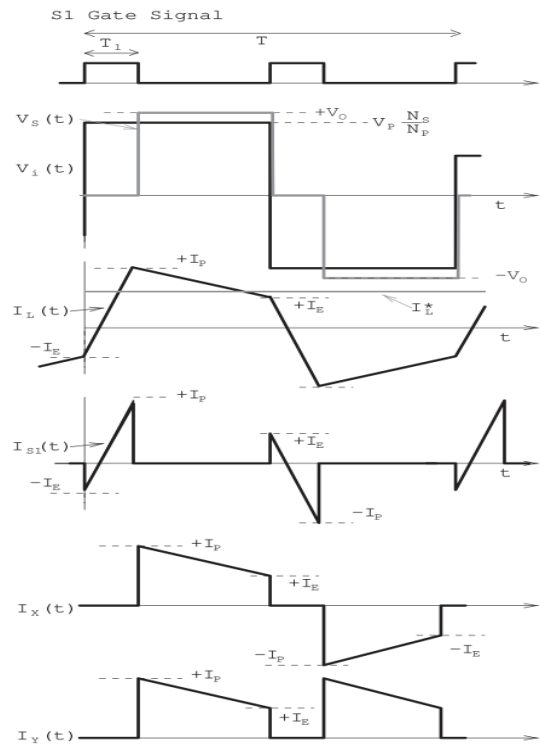
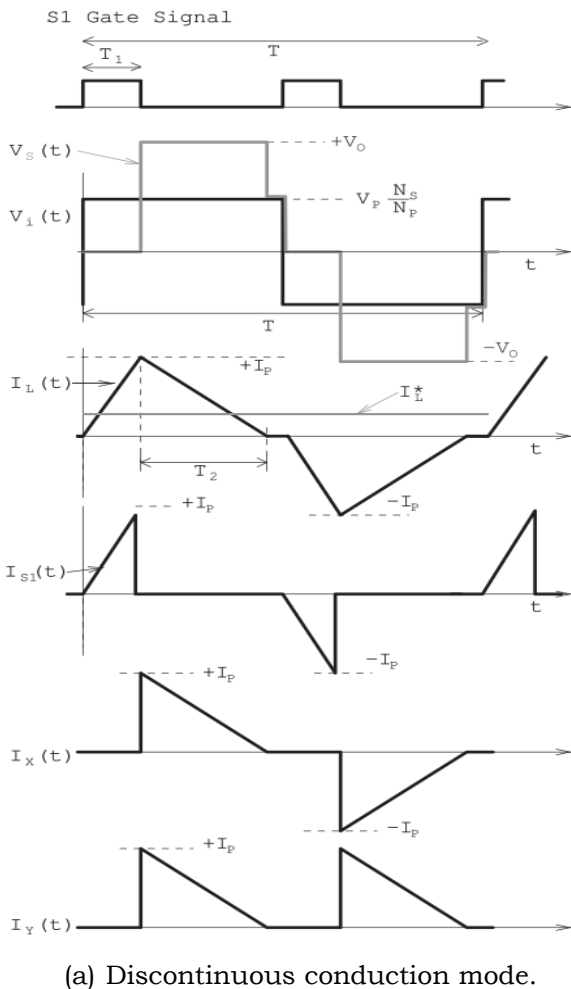


Fig. 3.3 Idealized waveforms. (a) Discontinuous conduction mode. (b) Continuous conduction mode.

### Power Handling Capability

The power capability of converter is determined by the maximum value of GM supported, which is limited by the requirement for (13) to result in a real number. This requires the argument under the square root to be non-negative, and hence

$$\frac{16G_{M\max} L_L V_I}{TV_O} \leq 1$$

$$P_{\max} = \frac{1}{2} G_{M\max} V_{I\max}^2 \text{ of}$$

$$P_{\max} \leq \frac{V_{AC} \frac{N_s}{N_p} V_O}{32\sqrt{2} f_s L_L}. \quad (3.14)$$

This equation can be used as a basis for converter design as demonstrated by the prototype example in Section V. The maximum peak current in the leakage inductor during the CCM can be calculated as follows:

$$I_{P\max} = \frac{V_O T}{8L_L} \quad (3.15)$$

And the transformer must be designed to handle this peak current without saturation.

### POWER SUPPLY CONTROL

The control objective for the power supply is to provide a constant output voltage and unity input power factor. This requires measurement of the output voltage and adjustment of the input current

through the GM factor defined in Section III-A. However, calculating the time parameter  $T_1$  in Section III-A and III-B also requires knowledge of the parameter  $L_L$ , the leakage

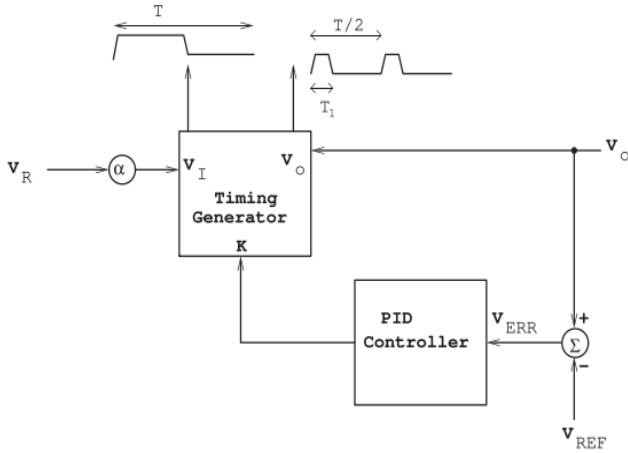


Fig. 3.4 Feedback control for the power supply. Inductance, which may not be accurately known. Therefore a new control parameter  $K$  is defined as follows:

$$K = \frac{G_M L_L}{T} \quad (3.16)$$

And  $K$  is used for control rather than  $GM$ . Substituting into (8) and (13) results in the required calculations for DCM as

$$T_1 = T \sqrt{K \left( \frac{V_O - V_I}{V_O} \right)} \quad (3.17)$$

And CCM as

$$T_1 = \frac{T}{4} \left( 1 - \sqrt{1 - \frac{16KV_I}{V_O}} \right) \quad (3.18)$$

It can further be shown that the boundary condition of (4) can be written as follows:

$$V_O(1 - 4K) \geq V_I \quad (3.19)$$

The feedback loop of Fig. 3.4 can then be used to control the power supply. In Fig. 3.4, the power supply output voltage  $V_O$  is measured and compared to a reference voltage  $V_{REF}$  to produce an output voltage error  $V_{ERR} = V_O - V_{REF}$ . This error voltage is used by a PID controller with dynamics below the input ac frequency  $f_{AC}$  to adjust the variable  $K$  to control the output voltage  $V_O$ .

The variable  $K$ , is used in the timing generator to generate the inverter timing and the secondary shorting period  $T_1$  twice per sample period  $T$ . The timing generator uses the measured power supply output voltage  $V_O$ , and a scaled version of the input rectifier voltage  $V_R$  as  $V_I = \alpha V_R$ . Using  $K$ ,  $V_I$ , and  $V_O$ , the timing generator evaluates the condition in (3.19) and if the result is true, the DCM is selected and (3.17) is used

to calculate the time period  $T_1$ . Otherwise, the CCM is selected and (3.18) is used to calculate the time period  $T_1$ .

## RESULTS AND DISCUSSION

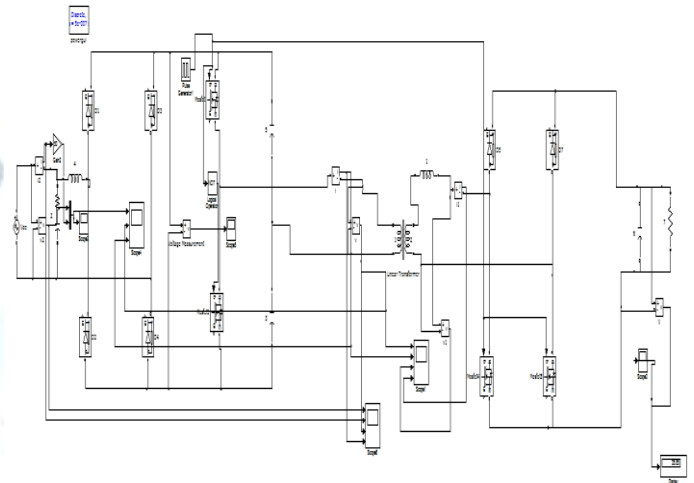


Fig 5.1 Simulink diagram of Proposed System Power Factor Corrected AC-DC power conversion

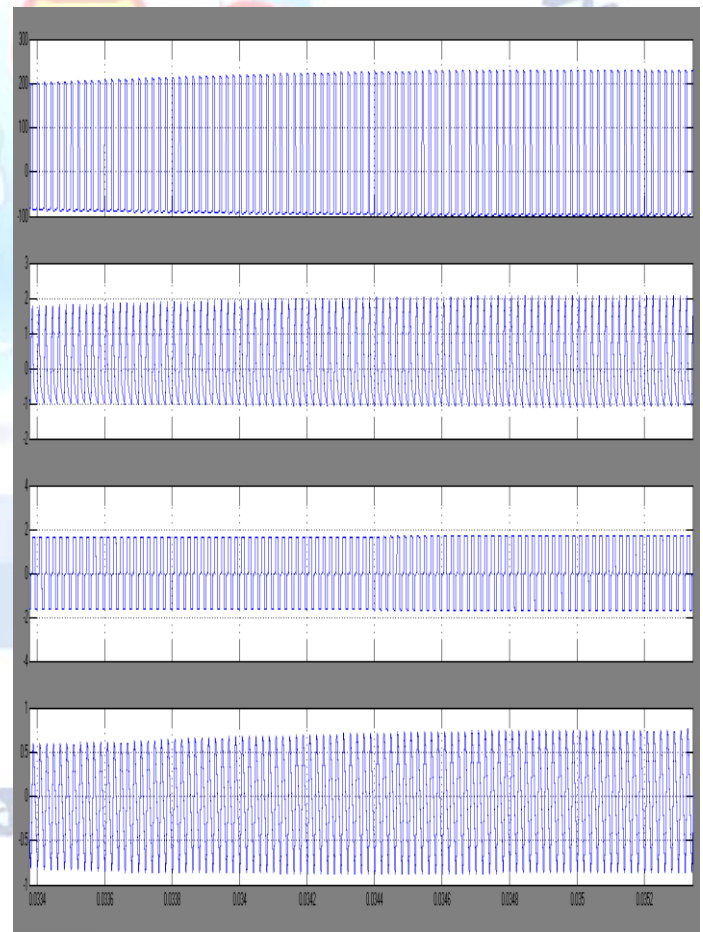


Fig. 5.2. Simulation waveforms at 300 W operation over a complete line cycle, input ac voltage (VAC) and current (IAC) and transformer primary voltage (VP) and current (IP)

Measured waveforms of the line input voltage and current and transformer primary voltage and current are shown in Fig. 5.2 over a full line cycle. Zoomed in waveforms of the transformer primary voltage and current and secondary voltage and current are shown in Fig. 5.3 (DCM) and Fig. 5.4 (CCM) and confirm the desired operation. The effect of finite values of bus capacitors C1 and C2 can be seen in the primary voltage waveform of Fig. 5.4 as a drop in the voltage rather than an ideal square wave.

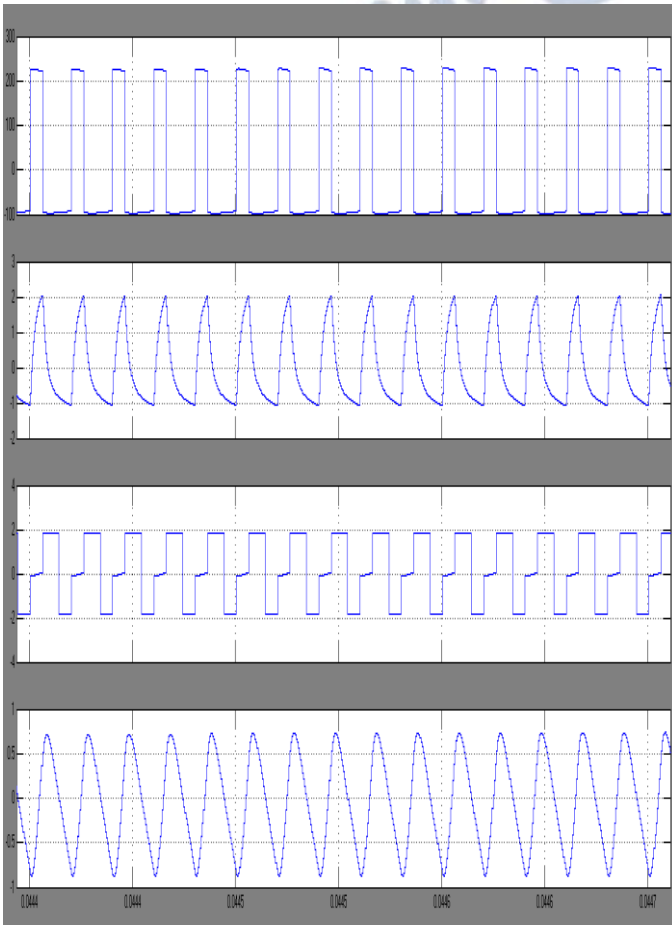


Fig. 5.3. Measured waveforms at 300 W operation, 1.5 ms from zero crossing and operating in DCM mode. Transformer primary voltage (VP) and current (IP) and secondary voltage (VS) and current (IS).

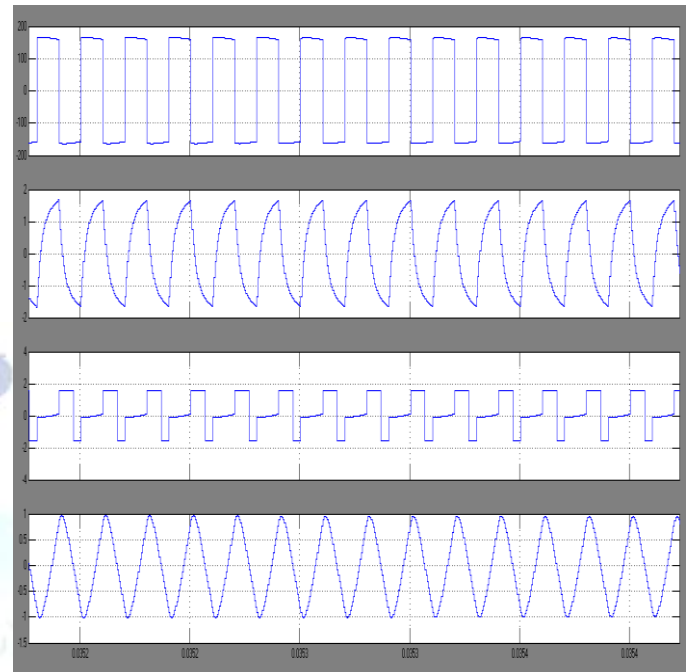


Fig. 5.4. Simulation waveforms at 300 W operation, 5 ms from zero crossing and operating in CCM mode. Transformer primary voltage (VP) and current (IP) and secondary voltage (VS) and current (IS).

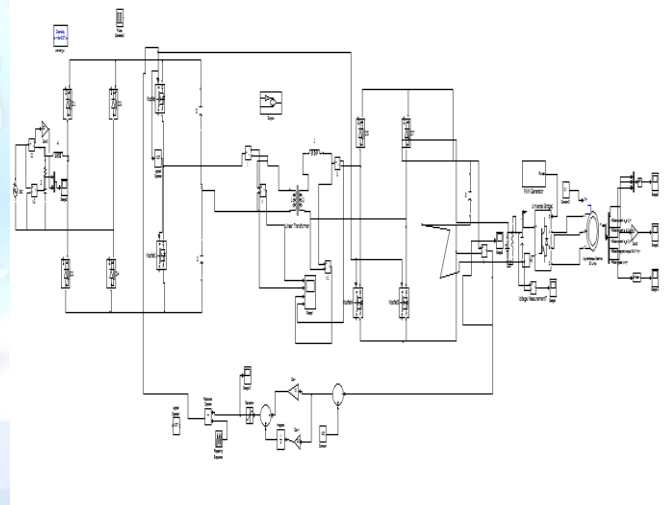


Fig 5.5 Simulink diagram of Proposed System Power Factor Corrected AC-DC power conversion with Induction Motor drive

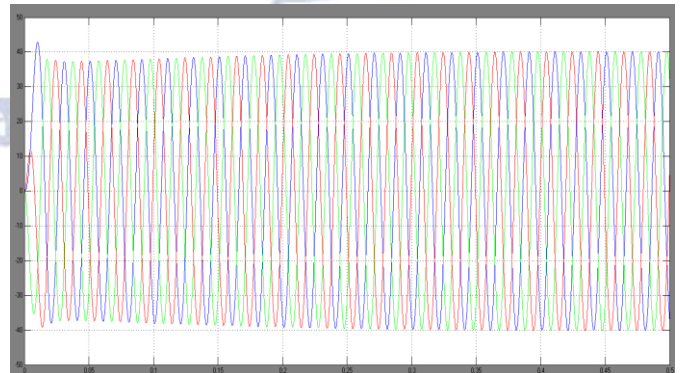


Fig 5.6 Simulation waveforms of Induction motor drive stator current characteristics

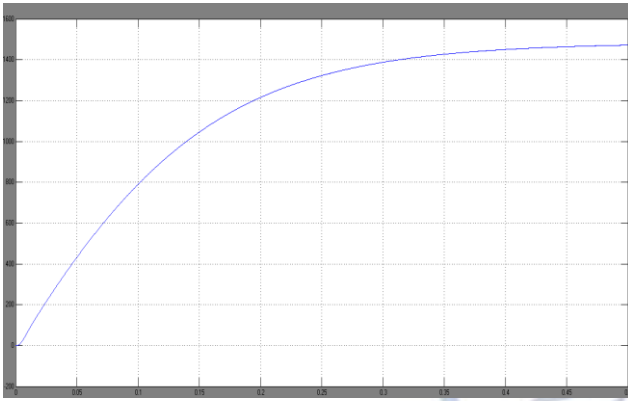


Fig 5.7 Simulation waveforms of Induction motor drive speed characteristics

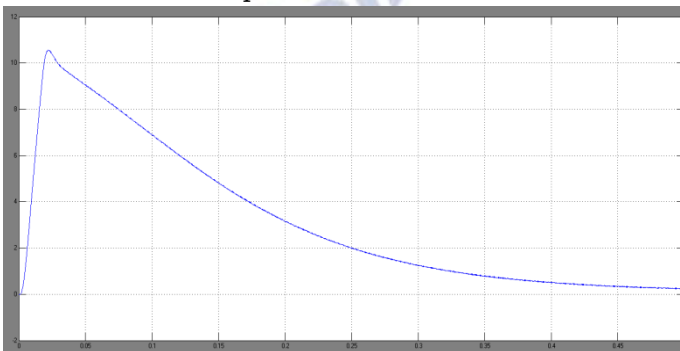


Fig 5.7 Simulation waveforms of Induction motor drive Torque characteristics

## CONCLUSION

This paper describes an isolated ac/dc power supply using the leakage inductance of the isolation transformer to achieve active power factor correction. The proposed with induction motor drive architecture allows for a compact lightweight power supply for power levels above that of flyback type PFC supplies. The principle of operation with two conduction modes is described and a timing based control method is developed for the power factor control. Measurements confirm the active power factor correction functionality with high power factor and low THD.

The proposed with induction motor drive power supply architecture is scalable and it should be feasible to extend the power capability of the proposed circuit to 500 W or more. Further variations on the principle can be adopted, such as universal input voltage operation, full bridge input inverter, zero current switching, synchronous rectification, interleaved designs, and so forth. The proposed architecture provides an additional option for the designers of PFC isolated supplies. And also verified the Induction motor characteristics.

## REFERENCES

[1] O. Garcia, J. A. Cobos, R. Prieto, P. Alou, and J. Uceda, "Single phase power factor correction: A survey," *IEEE*

*Trans. Power Electron.*, vol. 18, no. 3, pp. 749–755, May 2003.

[2] B. Singh, B. N. Singh, A. Chandra, K. Al-Haddad, A. Pandey, and D. P. Kothari, "A review of single-phase improved power quality AC-DC converters," *IEEE Trans. Ind. Electron.*, vol. 50, no. 5, pp. 962–981, Oct. 2003.

[3] M. M. Jovanovic and Y. Jang, "State-of-the-art, single-phase, active power factor correction techniques for high-power applications—An overview," *IEEE Trans. Ind. Electron.*, vol. 52, no. 3, pp. 701–708, Jun. 2005.

[4] N. Mohan, T. M. Undeland, and W. P. Robbins, *Power Electronics: Converters, Applications, and Design*. Hoboken, NJ, USA: Wiley, Oct. 2002.

[5] T. Yan, J. Xu, F. Zhang, J. Sha, and Z. Dong, "Variable-on-time-controlled critical-conduction-mode flyback PFC converter," *IEEE Trans. Ind. Electron.*, vol. 61, no. 11, pp. 6091–6099, Nov. 2014.

[6] D. G. Lamar, M. Arias, A. Rodriguez, A. Fernandez, M. M. Hernando, and J. Sebastian, "Design-oriented analysis and performance evaluation of a low-cost high-brightness LED driver based on flyback power factor corrector," *IEEE Trans. Ind. Electron.*, vol. 60, no. 7, pp. 2614–2626, Jul. 2013.

[7] C. Zhao, J. Zhang, and X. Wu, "An improved variable on-time control strategy for a CRM flyback PFC converter," *IEEE Trans. Power Electron.*, vol. 32, no. 2, pp. 915–919, Feb. 2017.

[8] J. W. Shin, S. J. Choi, and B. H. Cho, "High-efficiency bridgeless flyback rectifier with bidirectional switch and dual output windings," *IEEE Trans. Power Electron.*, vol. 29, no. 9, pp. 4752–4762, Sep. 2014.

[9] C.-P. Tung and H. S.-H. Chung, "A flyback AC/DC converter using power semiconductor filter for input power factor correction," in *Proc. IEEE Appl. Power Electron. Conf. Expo.*, Long Beach, CA, USA, 2016, pp. 1807–1814.

[10] L. Gu, W. Liang, M. Praglin, S. Chakraborty, and J. M. Rivas Davila, "A wide-input-range high-efficiency step-down power factor correction converter using variable frequency multiplier technique," *IEEE Trans. Power Electron.*, vol. 33, no. 11, pp. 9399–9411, Nov. 2018.

[11] K. Mino et al., "Novel bridgeless PFC converters with low inrush current stress and high efficiency," in *Proc. Int. Power Electron. Conf.—ECCEASIA*, Sapporo, Japan, 2010, pp. 1733–1739.

[12] M. Alam, W. Eberle, and N. Dohmeier, "An inrush limited, surge tolerant hybrid resonant bridgeless PWM AC-DC PFC converter," in *Proc. IEEE Energy Convers. Congr. Expo.*, Pittsburgh, PA, USA, 2014, pp. 5647–5651.

[13] A. H. Memon, K. Yao, Q. Chen, J. Guo, and W. Hu, "Variable-on-time control to achieve high input power factor for a CRM-integrated buck flyback PFC converter," *IEEE Trans. Power Electron.*, vol. 32, no. 7, pp. 5312–5322, Jul. 2017.

[14] H. S. Athab, D. Dah-Chuan Lu, A. Yazdani, and B. Wu, "An efficient single-switch quasi-active PFC converter with continuous input current and low DC-bus voltage stress," *IEEE Trans. Ind. Electron.*, vol. 61, no. 4, pp. 1735–1749, Apr. 2014.

[15] S. W. Lee and H. L. Do, "A single-switch AC-DC LED driver based on a boost-flyback PFC converter with lossless snubber," *IEEE Trans. Power Electron.*, vol. 32, no. 2, pp. 1375–1384, Feb. 2017.

[16] J. I. Baek, J. K. Kim, J. B. Lee, H. S. Youn, and G. W. Moon, "A boost PFC stage utilized as half-bridge converter for high-efficiency DC-DC stage in power supply unit," *IEEE Trans. Power Electron.*, vol. 32, no. 10, pp. 7449–7457, Oct. 2017.

- [17] M. A. Bakar and K. Bertilsson, "An improved modelling and construction of power transformer for controlled leakage inductance," in Proc. IEEE 16th Int. Conf. Environ. Elect. Eng., Florence, Italy, 2016, pp. 1–5.
- [18] R. Mitova, R. Ghosh, U. Mhaskar, D. Klikic, M. X. Wang, and A. Dentella, "Investigations of 600-V GaN HEMT and GaN diode for power converter applications," IEEE Trans. Power Electron., vol. 29, no. 5, pp. 2441–2452, May 2014.
- [19] A. M. Abou-Alfotouh, A. V. Radun, H. R. Chang, and C. Winterhalter, "A 1-MHz hard-switched silicon carbide DC/DC converter," IEEE Trans. Power Electron., vol. 21, no. 4, pp. 880–889, Jul. 2006.
- [20] J. S. Glaser et al., "Direct comparison of silicon and silicon carbide power transistors in high-frequency hard-switched applications," in Proc. 26th Annu. IEEE Appl. Power Electron. Conf. Expo., Fort Worth, TX, USA, 2011, pp. 1049–1056.
- [21] H. Wu, Y. Lu, T. Mu, and Y. Xing, "A family of soft-switching DC-DC converters based on a phase-shift-controlled active boost rectifier," IEEE Trans. Power Electron., vol. 30, no. 2, pp. 657–667, Feb. 2015.
- [22] C. A. Quinn and D. B. Dalal, "Empowering the electronics industry: A power technology roadmap," CPSS Trans. Power Electron. Appl., vol. 2, no. 4, pp. 306–319, Dec. 2017.

